Brillouin Study of the Quantization of Acoustic Modes in Nanospheres

M. H. Kuok,* H. S. Lim, S. C. Ng, N. N. Liu, and Z. K. Wang

Department of Physics, National University of Singapore, Singapore 117542, Republic of Singapore

(Received 3 January 2003; published 24 June 2003)

The vibrational modes in three-dimensional ordered arrays of unembedded SiO_2 nanospheres have been studied by Brillouin light scattering. Multiple distinct Brillouin peaks are observed whose frequencies are found to be inversely proportional to the diameter ($\approx$ 200–340 nm) of the nanospheres, in agreement with Lamb's theory. This is the first Brillouin observation of acoustic mode quantization in a nanoparticle arising from spatial confinement. The distinct spectral peaks measured afford an unambiguous assignment of seven surface and inner acoustic modes. Interestingly, the relative intensities and polarization dependence of the Brillouin spectrum do not agree with the predictions made for Raman scattering.

DOI: 10.1103/PhysRevLett.90.255502 PACS numbers: 63.22.+m, 62.30.+d, 62.65.+k, 78.35.+c

Low-dimensional systems exhibit interesting physical properties arising from spatial confinement effects, one of which is that their continuous energy spectrum is changed into a discrete one. In semiconductor quantum dots, electronic wave functions experience quantum confinement due to the dot boundary, inducing quantization of bulk electronic bands such that the quantum dots have electronic transitions that shift to higher energies with decreasing dot size [1]. In magnetic nanowires, bulk spin wave quantization has been observed using Brillouin light scattering [2]. In this study of nickel nanowire arrays, discrete modes which are a consequence of the quantization of bulk spin waves arising from confinement by the small cross section of the nanowires were observed.

Acoustic wave quantization in nanoparticles has been investigated by several groups using low-frequency Raman scattering [3–12]. The nanoparticles, ranging in size from a few to tens of nanometers, are in all cases embedded in a matrix. Results were analyzed based on the theory of acoustic modes confined in a homogeneous elastic sphere with a free surface, first formulated by Lamb [13] who predicted two categories of such modes, namely, the spheroidal and the torsional modes. They are labeled by the angular momentum quantum number l, where $l = 0, 1, 2, \ldots$ for spheroidal modes. However selection rules for light scattering derived by Duval [14] preclude the observation of torsional modes, while permitting only spheroidal modes with $l = 0$ or 2 to appear in the light scattering spectrum. The sequence of eigenmodes, in increasing order of energy, is indexed by n ($n = 1, 2, 3, \ldots$), where $n = 1$ corresponds to surface modes and values of $n \geq 2$ are associated with inner modes of the elastic sphere.

Samples used in the Raman studies are not particularly suited for the study of confined acoustic modes for the following reasons. First, the broad and poorly resolved spectra of these samples made mode assignment difficult. The particles studied were not perfectly spherical in shape nor were they monodisperse. These features gave rise to an undesirable broadening of the acoustic modes resulting in spectra that were not well resolved. In fact confined modes were not directly observed as individual spectral peaks but rather as component peaks obtained from the decomposition of broadbands. Second, analyses were complicated by the presence of the matrix surrounding the particles. This means that the stress-free boundary condition in the Lamb theory is not fulfilled. Effects due to the matrix include spectral line broadening [15], on top of that arising from the "imperfection" of particles mentioned above, and even suppression or elimination of surface modes [16]. Additionally, spectral peaks due to the matrix itself can obscure those of the sphere.

We found that synthetic opals, with their interconnected networks of ordered, close-packed SiO_2 nanospheres having diameters ranging from 200 to 340 nm, offer an excellent system for the investigation into the quantization of acoustic modes. One of their important applications is in their use as templates in the fabrication of photonic crystals [17]. Unlike earlier systems studied, the silica spheres are not embedded in any matrix, making synthetic opals a much simpler system to investigate. For instance, coupling of the spheres with the surrounding matrix medium does not exist here thus allowing us to apply Lamb's theory, which deals with spheres with a free surface, in the analysis of our results. Confined mode frequencies for particles in this size range fall within the gigahertz domain and Brillouin light scattering is ideally suited for the investigation of these modes. Scattering from these unembedded silica particles with a well-defined (near-perfect spherical) shape, and which are monodisperse (diameter deviation $<3\%$), produces well-resolved Brillouin spectra. These spectral features afforded the detection of confined modes of $n = 1, 2, 3$, and 4, the highest number of inner modes measured so far.

The samples studied are in the form of synthetic opals obtained from JSC Opalon. They are composed of highly ordered arrays of amorphous SiO_2 nanospheres arranged in a face-centered cubic lattice. Our scanning electron microscope (SEM) images (Fig. 1) reveal that each

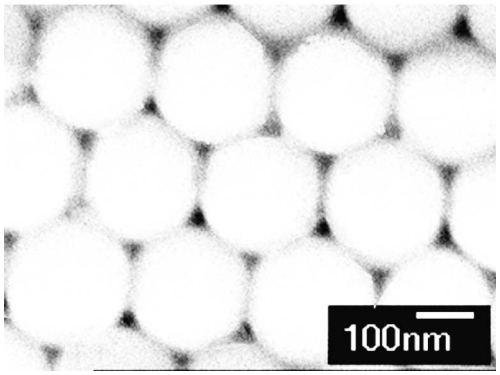

FIG. 1. Scanning electron microscope image of a synthetic opal sample comprising highly ordered monodisperse SiO_2 spheres of 204 nm diameter.

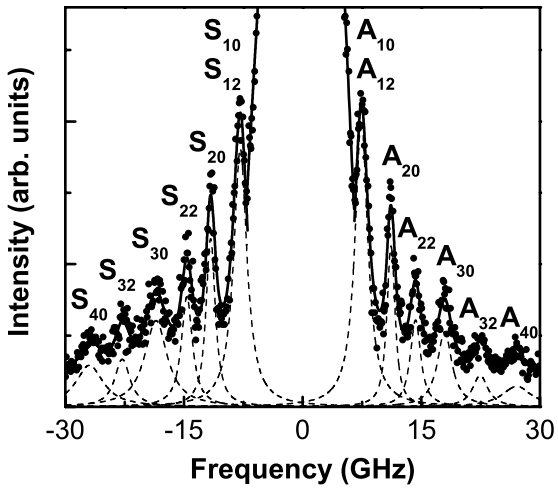

FIG. 2. A typical p-p polarized Brillouin spectrum of the 340 nm-diameter SiO_2 nanosphere sample. Experimental data are denoted by dots. The spectrum is fitted with Lorentzian functions (dashed curves) and the resultant fitted spectrum is shown as a solid curve. S_{nl} and A_{nl} denote the respective Stokes and anti-Stokes peaks arising from confined acoustic modes in the nanospheres.

sample consists of near-perfect spheres of the same diameter; samples with nanosphere diameters of 204, 237, 284, and 340 nm ($\pm$ 3%) were studied. Brillouin spectra were recorded at room temperature in the 180°-backscattering geometry using a (3 + 3)-pass tandem Fabry-Pérot interferometer equipped with a silicon avalanche diode detector and the 514.5 nm line of an argon-ion laser. The laser light was incident on the top surface of each sample such that the surface normal lies in the scattering plane.

Figure 2 shows the p-p polarized Brillouin spectrum recorded at an incident angle of 70°, of a 340 nm-diameter SiO_2 nanosphere sample. It features six well-separated Brillouin peaks lying between about 7–27 GHz. Similar spectra were obtained for spheres of other diameters. It is noteworthy that the frequencies and relative intensity of these peaks are independent of polarization and the incident angle. Additionally the Brillouin spectrum is independent of the in-plane orientation of the samples. These observations imply that the six spectral peaks observed arise from the acoustic modes of individual nanospheres rather than those of the bulk sample. The resulting Brillouin frequencies were plotted as a function of inverse nanosphere diameter in Fig. 3 which clearly reveals their linear dependence.

The eigenvalue equation [16,18] for the spheroidal mode (for $l \geq 0$) is

$$2\left[\eta^2 + (l-1)(l+2)\left(\frac{\eta j_{l+1}(\eta)}{j_l(\eta)} - (l+1)\right)\right]\frac{\xi j_{l+1}(\xi)}{j_l(\xi)} -$$

$$\frac{1}{2}\eta^4 + (l-1)(2l+1)\eta^2 + [\eta^2 - 2l(l-1)(l+2)]\frac{\eta j_{l+1}(\eta)}{j_l(\eta)} = 0, \quad (1)$$

where ξ and η are the eigenvalues, and $j_l(\eta)$ the spherical Bessel function of the first kind. The eigenvalues can be expressed as

$$\xi_{nl} = \pi\nu_{nl}D/V_L \quad \text{and} \quad \eta_{nl} = \pi\nu_{nl}D/V_T, \quad (2)$$

where ν_{nl} is the spheroidal mode frequency; V_L and V_T are the respective longitudinal and transverse sound velocities.

The eigenvalues for each l depend on only the two independent bulk parameters, V_L and V_T, which were found by fitting the calculated frequencies ν_{nl}, obtained from Eqs. (1) and (2), to the experimental ones ν_{nl}^{expt} to minimize the residual R ($= \sum_{n,l}[\nu_{nl} - \nu_{nl}^{\text{expt}}]^2$). The summation involves only the following four modes: $(n, l) =$ (1, 0), (2,0), (2,2), and (3,0). These modes were chosen as they appear as sharper Brillouin peaks and hence their frequencies were measured with a higher precision. Next, a two-dimensional mesh for the two parameters was created, and the residual, R, computed at each point on the mesh. The optimal fit corresponded to the smallest R. Fitting yielded longitudinal and transverse acoustic mode velocities of $V_L = 5279$ m/s and $V_T = 3344$ m/s, respectively. The Young's modulus and Poisson ratio of our SiO_2 nanospheres estimated from these velocities are 57.3 GPa and 0.17, based on a density of 2.2×10^3 kg/m^3 for bulk synthetic silica glass [19]. These values are reasonably close to the Young's modulus and Poisson ratio of 72.9 GPa and 0.17, respectively, measured by Comte and von Stebut, for bulk fused silica [20]. The

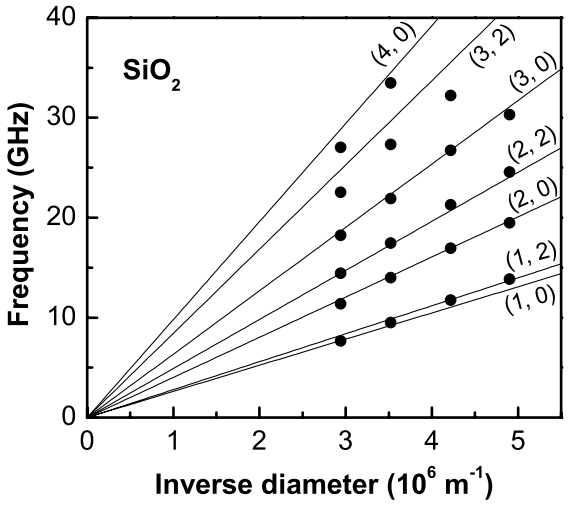

FIG. 3. Dependence of Brillouin peak frequency on the inverse nanosphere diameter. Experimental data are denoted by dots. The lines represent the theoretical frequencies, ν_{nl}, given by Eq. (3), for various modes labeled by (n, l).

calculated frequencies ν_{nl} (in GHz) are given by

$$\nu_{10} = \frac{2.617}{D}, \quad \nu_{12} = \frac{2.796}{D}, \quad \nu_{20} = \frac{4.017}{D}, \quad \nu_{22} = \frac{4.098}{D}, \quad \nu_{30} = \frac{6.343}{D}, \quad \nu_{32} = \frac{8.427}{D}, \quad \nu_{40} = \frac{9.804}{D}, \tag{3}$$

where D is the diameter of the sphere (in 10^{-6} m). Reference to Fig. 3 shows that there is excellent agreement between the calculated and measured values of the frequencies. One interesting feature is the proximity of the two lowest-gradient lines corresponding to the respective $(n = 1, l = 0)$ and $(n = 1, l = 2)$ modes to which the same lowest-frequency Brillouin peak is assigned. This narrow peak could not be resolved into two modes.

It is noteworthy that measurements made in *p-p* and *p-s* polarization configurations yielded Brillouin spectra that are identical, in contradiction with the prediction made by Duval [14] for Raman scattering. He found that spheroidal modes with $l = 0$ produce only polarized (*p-p*) Raman spectra, while those with $l = 2$ give both polarized and depolarized (*p-s*) ones. Furthermore, our measured relative intensities differ from the theoretical ones calculated by Montagna and Dusi [15]. For instance, for the spheroidal $l = 0$ mode, the calculated intensity ratio of the $n = 2$ to the $n = 1$ mode of 0.12 is much smaller than our measured ratio. There are major differences between our Brillouin scattering and the Raman scattering experiments. In the former, the size of the spheres is of the same order of the excitation light wavelength, while in the latter, it is much smaller. The theoretical calculations of Duval [14] as well as Montagna and Dusi [15] are based on the assumption of the sphere diameter being much shorter than the excitation light wavelength. The invalidity of this assumption in our case could account for the discrepancies between our Brillouin observations and the theoretical Raman predictions.

In summary, we report the first observation, by Brillouin light scattering, of multiple acoustic modes in three-dimensional ordered arrays of matrix-free SiO_2 nanospheres. Our analysis, based on the Lamb theory, indicates that the discrete modes observed are a consequence of the quantization of acoustic modes due to spatial confinement by the nanospheres. A combination of the following features of the nanospheres in the present study — near-perfect spherical shape, monodisperse, and matrix-free environment — affords the detection of up to seven confined acoustic modes, thus providing clear evidence of acoustic mode quantization in a nanometer-size particle.

The authors are grateful to H. K. Wong and P. M. Ong for providing the SEM data.

*Corresponding author.
Email address: phykmh@nus.edu.sg

[1] D. J. Norris, A. Sacra, C. B. Murray, and M. G. Bawendi, Phys. Rev. Lett. **72**, 2612 (1994).
[2] Z. K. Wang, M. H. Kuok, S. C. Ng, D. J. Lockwood, M. G. Cottam, K. Nielsch, R. B. Wehrspohn, and U. Gösele, Phys. Rev. Lett. **89**, 027201 (2002).
[3] A. Tanaka, S. Onari, and T. Arai, Phys. Rev. B **47**, 1237 (1993).
[4] M. Fujii, Y. Kanzawa, S. Hayashi, and K. Yamamoto, Phys. Rev. B **54**, R8373 (1996).
[5] E. Duval, A. Boukenter, and B. Champagnon, Phys. Rev. Lett. **56**, 2052 (1986).
[6] M. Ikezawa, T. Okuno, Y. Masumoto, and A. A. Lipovskii, Phys. Rev. B **64**, 201315 (2001).
[7] P. Verma, W. Cordts, G. Irmer, and J. Monecke, Phys. Rev. B **60**, 5778 (1999).
[8] L. Saviot, B. Champagnon, E. Duval, I. A. Kudriavtsev, and A. I. Ekimov, J. Non-Cryst. Solids **197**, 238 (1996).
[9] E. P. Denisov, S. V. Karpov, E. V. Kolobkova, B. V. Novikov, A. I. Suslikov, D. L. Fedorov, and M. A. Yastrebova, Phys. Solid State **41**, 1194 (1999).
[10] A. Roy and A. K. Sood, Solid State Commun. **97**, 97 (1995).
[11] A. Dieguez, A. Romano-Rodriguez, A. Vila, and J. R. Morante, J. Appl. Phys. **90**, 1550 (2001).
[12] P. Nandakumar, C. Vijayan, M. Rajalakshmi, A. K. Arora, and Y. V. G. S. Murti, Physica (Amsterdam) **11E**, 377 (2001).
[13] H. Lamb, Proc. London Math. Soc. **13**, 189 (1882).
[14] E. Duval, Phys. Rev. B **46**, 5795 (1992).
[15] M. Montagna and R. Dusi, Phys. Rev. B **52**, 10 080 (1995).
[16] A. Tamura, K. Higeta, and T. Ichinokawa, J. Phys. C **15**, 4975 (1982).

[17] Y. A. Vlasov, X. Z. Bo, J. C. Sturm, and D. J. Norris, Nature (London) **414**, 289 (2001).
[18] N. Nishiguchi and T. Sakuma, Solid State Commun. **38**, 1073 (1981).
[19] J. Kushibiki, M. Arakawa, and R. Okabe, IEEE Trans. Ultrason. Ferroelectr. Freq. Control **49**, 827 (2002).
[20] C. Comte and J. von Stebut, Surf. Coat. Technol. **154**, 42 (2002).